Comparative study on alloy cluster formation in Co-Al and Co-Pt systems

Toyohiko J. Konno and Saeki Yamamuro[a)]
Institute for Materials Research, Tohoku University, Sendai 980-8577, Japan

Kenji Sumiyama
Department of Materials Science and Engineering, Nagoya Institute of Technology, Nagoya 466-8555, Japan

The formation of alloy clusters using a plasma-gas-aggregation technique is described for Co-Al and Co-Pt systems. This method employs two separate elemental sputtering sources and a growth chamber. Metallic vapors generated were cooled rapidly in an Ar atmosphere, and grown into alloy clusters. The composition of the clusters was controlled by adjusting the ratio of the applied sputtering power. We found that B2-CoAl clusters of about 12 nm in diameter were formed for a composition range wider than that predicted by the Co-Al phase diagram, and that high-temperature fcc-CoPt clusters were formed in the Co-Pt system. These findings suggest the nonequilibrium nature of the cluster formation. The size distribution of the clusters is highly monodispersive and does not follow commonly observed log-normal distribution. These results were discussed from the viewpoint of simple gas dynamics. We concluded that monomer absorption with discrete residence time is the dominant mechanism for monodispersive alloy cluster formation, and that the contrasting thermodynamical features between the Co-Al and Co-Pt systems are at the cause of the observed difference in average cluster size. © *2002 American Vacuum Society.* [DOI: 10.1116/1.1470518]

I. INTRODUCTION

Reports on the production of small metallic particles in the gaseous phase date back a long time.[1,2] The most well-known method consists of the simple evaporation of a metal. The evaporated metallic atoms are cooled in an inert gas atmosphere by repeated collisions with a carrier gas, following which they grow into a cluster.[3–6] This method of generating clusters is broadly known as the gas-aggregation technique. Recently, methods, such as sputtering or laser ablation, have been employed as a source of metallic gas.[7–10] Irrespective of the metallic vapor generation method used, however, cluster formation is essentially an irreversible process. Various experiments and discussions have focused on how a cluster or a small particle nucleates and grows.[11–14] For example, Katz discussed homogeneous nucleation from a supersaturated vapor,[15] while Granqvist and Buhrman explained the emergence of the log-normal distribution (LND), as opposed to the normal Gaussian distribution, of particle sizes.[16]

Most of the systems examined so far, experimentally or theoretically, have been limited to the formation of organic or pure metal clusters. Needless to say, however, when a metal forms an alloy with another kind of metal, the stability of the alloy phase depends heavily on the kind of compound formed. While elemental metal clusters[17,18] and their oxides[19,20] have been widely studied, so far very little research has focused on the formation of alloy clusters by the gas aggregation technique. Yukawa *et al.* studied the formation of Cr-based alloy particles, which was mainly triggered by the presence of metastable δ-Cr (A15-type in Structure

Bericht notation), and its extent when mixed with other metals.[21]

In addition to the scientific aspects of the formation of alloy clusters, clusters comprising intermetallic compounds are of practical interest. For example, ferromagnetic alloy clusters are expected to exhibit excellent magnetic properties, such as large coercivity, because of the large magnetic anisotropy and the small size of the particles.[22,23] Furthermore, it should be mentioned that Wang *et al.* reported alloy cluster formation in the Pt-Sn and Su-Sn systems by using cold organic solvents for catalytic application. In this way, they succeeded in kinetically controlling the size distribution and surface ligation of the alloy clusters.[24] In view of the scientific and technological importance of such findings, further studies on alloy cluster formation by the gas-aggregation method need to be carried out.

In the present investigation, we compared the alloy forming behaviors in the Co-Al and Co-Pt binary systems.[25,26] These two systems were selected because they possess an intermetallic compound phase near the composition range of Co:M=1:1 (M=Al or Pt).[27,28] Furthermore, the free energy change, ΔG, upon the formation of the CoAl phase (B2) is much larger than that of CoPt (L1$_0$),[29] thus allowing us to examine the effect of the stability of the alloy phase on the kinetics of cluster formation. Table I summarizes some of the contrasting features between the two intermetallic alloys. Experimentally, the relative and absolute amount of two kinds of metallic vapors cannot be controlled easily with conventional evaporation methods that rely on the temperature of crucibles to generate individual metallic vapors. Moreover, the drawback of a sputter-based method employing a single alloy target is that it involves cumbersome preparation of alloy materials, which are often difficult to process mechani-

[a)]Current address: Department of Physics, Carnegie-Mellon University, Pittsburgh, PA 15213.

TABLE I. Structure and heat of formation of CoM (M=Al or Pt) intermetallic compounds.

	Structure	Lattice constant (Refs. 27 and 28) (Å)	Heat of formation for CoM (M=Al, Pt) (Ref. 29) (kJ/mol)	Maximum temperature for CoM (°C)
CoAl	B2	$a=2.86$	-60	1645
CoPt	$L1_0$	$a=3.79, c=3.69$	-14	825

cally. We thus employed a two-target sputtering system in order to generate and control independently the amounts of Co and Al (or Pt) metallic vapors. It was not immediately obvious with this method, however, that the two kinds of metal vapors generated from the two sources placed apart (about 10 cm) could actually mix, react, and form an alloy in a gas phase. Our results indicate that it is indeed possible to fabricate monodispersive alloy clusters this way for a relatively wide composition range in a controlled manner, and that the size, composition, and product phases depend heavily on the thermodynamical aspect of the alloy system.

II. EXPERIMENTAL PROCEDURE

Figure 1 depicts an experimental setup for cluster formation using the sputter-based gas-aggregation technique.[10,30] We used two independently powered sputtering targets for the generation of pure metal vapors. The two targets were placed face to face, 10 cm apart, and the input power of each target was controlled in the range of 100–300 W. A large amount of Ar gas of 200–400 standard cubic centimeters per minute (sccm) was introduced continuously into the sputtering chamber, raising the pressure inside the chamber to approximately 130 Pa. This unusually high Ar pressure restricted the glow discharge region to only a few millimeters above each target, allowing independent control over the power of the targets despite the fact that these were placed face to face. One of the advantages of this configuration is that the different elements can mix effectively. During sputtering, the applied voltage remained constant at approxi-

mately 300 V for each target, irrespective of the applied power: it is the current, within a range of about 0.33–1 A, that changes according to the applied power. It should be emphasized here that the sputter yield ratio of Al to Co is approximately 0.86, while that of Pt to Co is approximately 1.14 (Table II).[31] Thus, the same amount of power applied to Al or Pt should result in different amounts of metal vapors, i.e., the amount of Pt vapor should be larger than that of Al produced under the same conditions. Table II also shows mass and energy transfer function (for collision with Ar) of the elements involved. The latter is given by

$$4m_{Ar}m_M/(m_{Ar}+m_M)^2, \tag{1}$$

where m_{Ar} and m_M are the mass of Ar and colliding atom (Co, Al, Pt, or Ar), respectively.[32] The metal vapors thus generated were swept into the growth region (approximately 5 cm in diameter and 20 cm in length, set at the liquid nitrogen temperature), with an Ar carrier gas. There was also an aperture of the same size at the exit of the growth region. The clusters coming out of the aperture were led to the deposition chamber, which was kept below about 1×10^{-2} Pa through two skimmers by differential pumping. The clusters were finally deposited on carbon-coated colodion films supported by Cu grids at room temperature for transmission electron microscopy (TEM) observations. We used a Hitachi HF-2000 transmission electron microscope operating at 200 kV for structural characterization. This microscope was equipped with x-ray energy dispersive spectroscopy (EDS), which was used for compositional analyses.
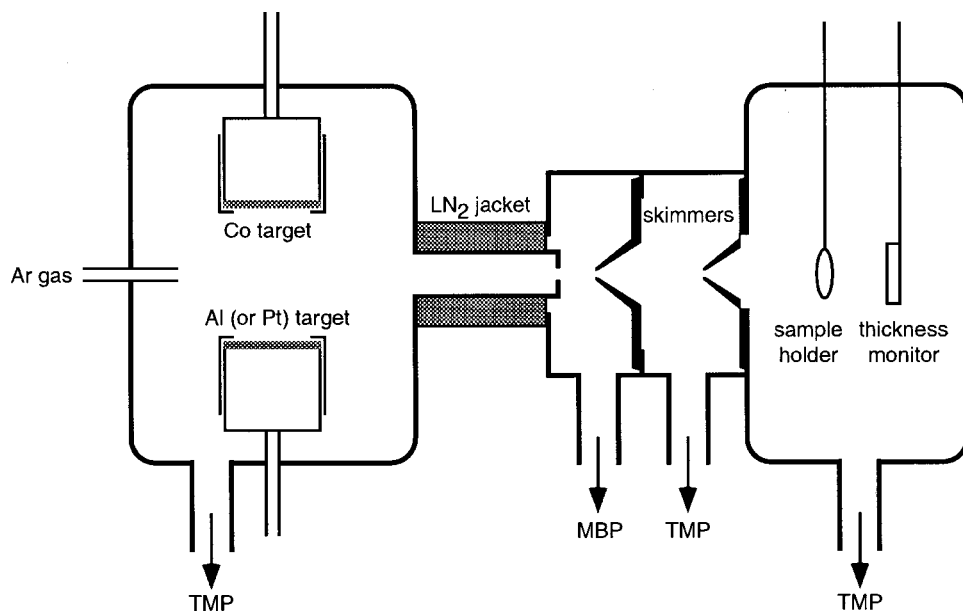

FIG. 1. Schematic drawing of the chamber for the preparation of alloy clusters: the plasma-gas-aggregation system. Two kinds of metallic vapors, generated by sputtering the targets placed face-to-face, are mixed and cooled, giving rise to uniformly sized alloy clusters. They are transported by an Ar carrier gas through two skimmers by differential pumping, and finally deposited on a substrate. (TMP: turbo-molecular pump; MBP: mechanical booster pump.)

TABLE II. Mass, sputtering yield, and energy transfer function with the collision of Ar for Co, Al, Pt, and Ar.

	Mass	Sputtering yield (by Ar ion) (Ref. 31)	Energy transfer function (against Ar)
Co	58.9	1.22	0.963
Al	27.0	1.05	0.963
Pt	195.1	1.40	0.564
Ar	39.9		1

III. EXPERIMENTAL RESULTS

A. Cluster size distribution

Figure 2 shows bright-field TEM micrographs of (a)–(c) Co-Al and (d)–(e) Co-Pt clusters. In this particular series of experiments, the sputtering power of Al (or Pt) was fixed to 100 W, while that the Co target varied from 100, 200, and 300 W at a fixed Ar gas flow rate of 300 sccm. As seen, the size of the produced clusters is uniform in each condition, but the average size, which ranges from 5 to 20 nm in diameter, depends heavily on the alloy system and applied power of the Co target.

Figure 3 shows the size distribution of (a)–(e) Co-Al and (f)–(j) Co-Pt clusters prepared under various conditions including those shown in Fig. 2. For each condition, more than 100 clusters were randomly selected to obtain the distribution. (Overlapping images of clusters were rejected from the selections.) As can be seen, except for (a) and (b), the distributions do not follow LND, but the normal Gaussian distribution with a small standard deviation σ, and thus may be called monodispersive. We also observe a general trend where Co-Al clusters are larger than Co-Pt clusters. In addition, the average size of the Co-Al clusters decreases with the sputtering power of Co, while the opposite occurs for the Co-Pt clusters.

Figure 4 summarizes the average composition of the clusters determined by EDS analysis. The electron beam was spread with a diameter of more than 500 nm, and thus the values in the figure represent the average composition of the cluster aggregates. We also measured the composition of individual clusters, and found that, except for Al-rich clusters,[33] the composition of each cluster did not vary by more than 5%, corresponding to the experimental error margin of EDS. As shown, the composition of the clusters can be controlled easily by changing the relative power of the two targets. As expected, the Co content of the clusters increased as the applied power to the Co target increased. Contrary to our expectations, however, the Co-Pt alloy clusters were richer in Co than the corresponding Co-Al alloy clusters produced under the same conditions, despite the fact that the sputtering yield of Pt was greater than that of Al. It was also found that the average composition was a strong function of another processing parameter: Ar gas flow rate. We found that increasing the rate from 300 to 500 sccm resulted in Co-Pt clusters that are rich in Pt, as indicated by the crosses in the figure. These observations suggest that both thermodynamics and kinetics of cluster formation plays an impor-
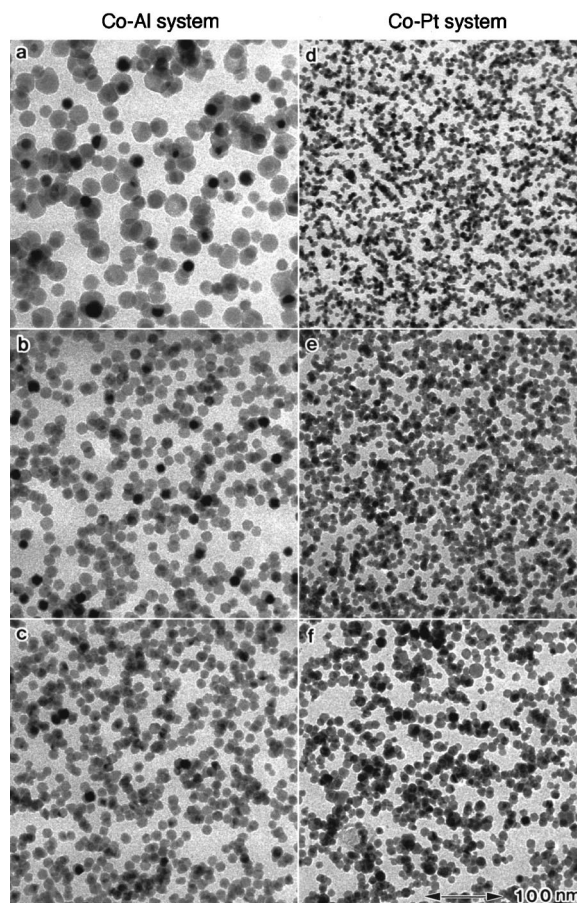

FIG. 2. Bright field TEM micrographs of alloy clusters, produced with the following condition: Ar gas flow rate: 300 sccm (fixed); (a), (b), and (c) Co-Al system with sputtering power of Co (SP_{Co})=100, 200, and 300 W, respectively, and SP_{Al}=100 W (fixed); (d), (e), and (f) Co-Pt system with SP_{Co}=100, 200, and 300 W, respectively, and SP_{Pt}=100 W (fixed).

tant role in determining the composition of the produced cluster aggregates.

B. Structure of clusters

Figure 5 shows typical electron diffraction (ED) patterns of the cluster aggregates in Co-Al [(a)–(c)] and Co(Pt) [(d)–(f)] systems. The diffraction rings in the ED pattern (a) taken for Co:Al=23.77 can be indexed as those for the fcc-Al phase with a=4.05 Å. On the other hand, the diffraction rings indicated by the arrowheads in the ED pattern (b) can be indexed as {100}, {111}, and {210} of simple cubic structure, and show that the clusters with the composition of Co:Al=54.46 possess the B2 (CsCl) structure. The lattice constant obtained from the ED pattern was 2.85 ± 0.02 Å, in agreement with the lattice constant of the CoAl(B2) phase, 2.86 Å.[27] As the Co content of the cluster aggregates increases in the Co-Al system, the ED patterns suggest that the clusters begin to assume the fcc-Co phase, in which Al is presumably dissolved. Figure 4(c) is the ED pattern taken for Co:Al=76.24. Here, the rings can be identified as arising from the B2(CsCl) structure, as well as from the fcc-Co
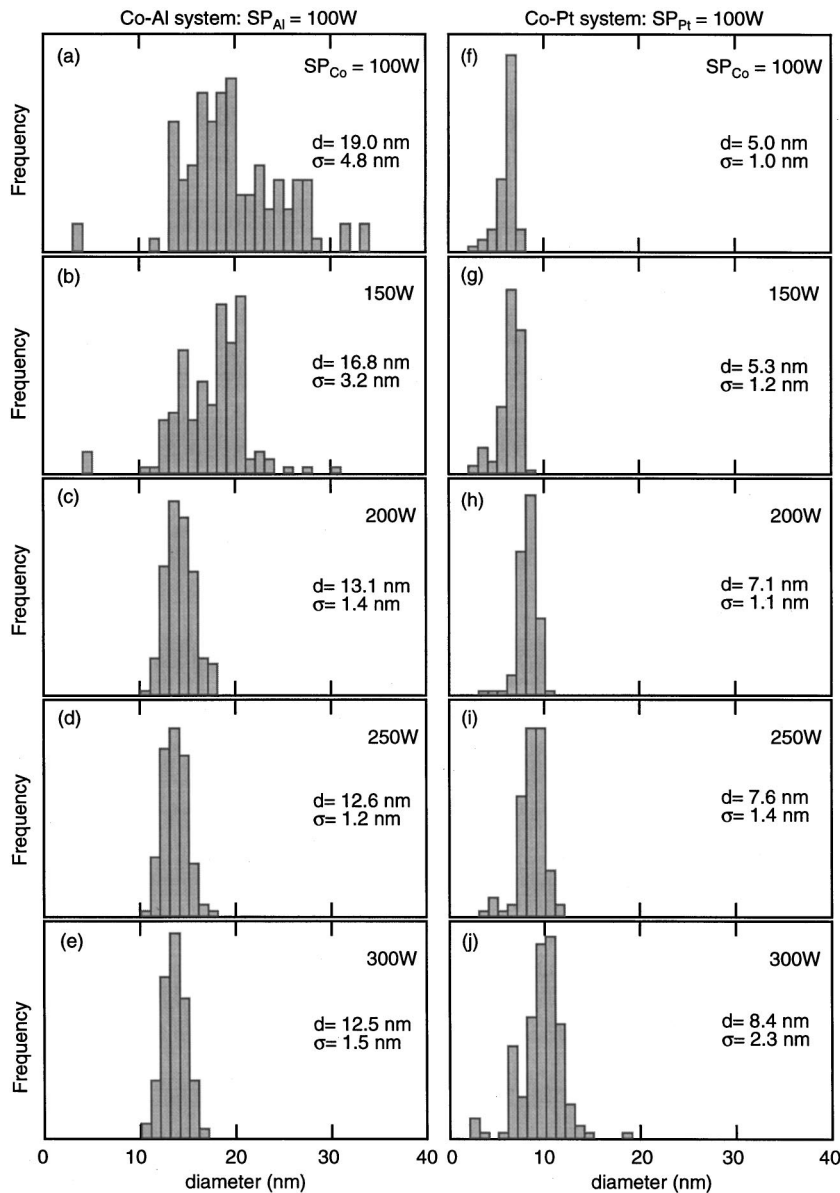
FIG. 3. Size distribution of alloy clusters. Ar gas flow rate: 300 sccm. (a)–(e) Co-Al system; (f)–(j) Co-Pt system. $SP_{Al} = SP_{Pt} = 100$ W (fixed), while SP_{Co} was varied as indicated. d: average diameter; σ: standard deviation as defined for the normal Gaussian distribution, Eq. (3). Approximately 100 clusters were randomly sampled for each condition.

phase with $a = 3.54$ Å. This shows that in the Co-rich region the clusters form a two-phase comprising the CoAl(B2) phase and the fcc-Co phase.

Figures 5(d) and 5(e) are the ED patterns of cluster aggregates with Co:Pt=38.62 and Co:Pt=64:36, respectively. These ED patterns are typical of the fcc structure and show that the clusters possess the fcc-Co phase, in which Pt is dissolved. No intermetallic phase, such as the $L1_0$-type that exists in the equilibrium phase diagram, was observed. On the other hand, the diffraction rings in the ED pattern shown in Fig. 4(f), which was taken from the Co:Pt=79:21 cluster aggregates, cannot be indexed as arising from the fcc-Co phase, but rather from the hexagonal close-packed (hcp) Co phase. This observation shows the hcp-Co is stabilized by the incorporation of Pt atoms, in agreement with the behavior reported in the literature.[34]

Figure 6 summarizes the size and structure of the Co-Al and Co-Pt alloy clusters as a function of their Co contents.

The clusters were produced under the following conditions: Ar flow rate was fixed at 300 sccm; sputtering power of Al (or Pt) was fixed at 100 W; sputtering power of Co was varied from 100 to 300 W. As shown here, the size of the Co-Al alloy clusters is generally larger than that of the Co-Pt alloy clusters despite the fact that the sputtering conditions are almost the same. In addition to the large asymmetry of the average size between the two alloy systems, we note that the observed phase in both systems differs from that expected from the respective equilibrium phase diagrams. For example, the Co-Al phase diagram shows that Co atoms can dissolve in the B2 phase only up to about 56 at %-Co at 300 °C, while at 1200–1450 °C the ordered B2 phase can exist in a wide composition range, i.e., about 46 at %-Co to more than 70 at %-Co.[25] Thus, the composition range in which the B2 structure is found in the present article corresponds to a state at a high temperature. Likewise, the Co-Pt phase diagram shows that the $L1_0$ phase is stable below
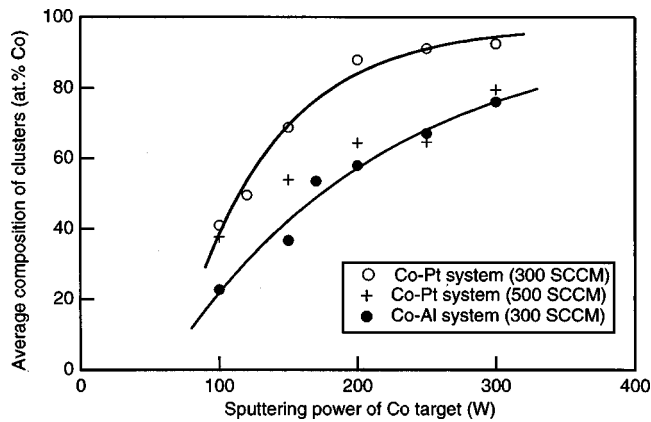
FIG. 4. Average composition of clusters as a function of SP_{Co}, with $SP_{Al} = SP_{Pt} = 100$ W (fixed), showing that the Co contents of clusters increases with increasing SP_{Co}. Note, however, that the Co-Pt clusters become richer in Co than the corresponding Co-Al clusters produced under the identical conditions, despite the fact that the sputtering yield of Pt is larger than that of Al. Increasing the Ar gas flow rate from 300 to 500 sccm suppresses the Co content of the Co-Pt clusters.

FIG. 5. Electron diffraction patterns of alloy clusters with the average composition of (a) $Co_{23}Al_{77}$, (b) $Co_{54}Al_{46}$, (c) $Co_{76}Al_{24}$, (d) $Co_{41}Pt_{59}$, (e) $Co_{69}Pt_{31}$, and (f) $Co_{80}Pt_{20}$. In the Co-Al system, diffraction rings indicated by the arrowheads in (b) suggests the formation of intermetallic CoAl compound (B2 structure), while the diffraction rings of the Al-rich (a) and Co-rich (c) clusters are dominated by the fcc Al and fcc Co phase, respectively. In the Co-Pt system, diffraction rings in (d) and (e) can be identified as those of the fcc Co phase, while the rings in (f) suggests the formation of hcp Co phase.
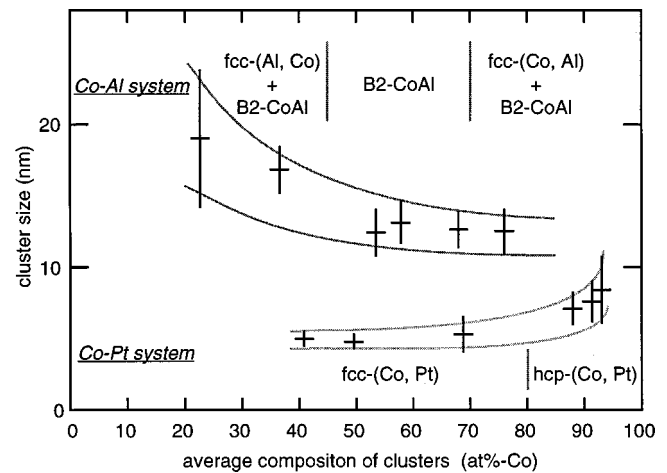
FIG. 6. Size (average diameter and standard deviation) of Co-Al and Co-Pt alloy clusters and their structure as a function of Co contents.

825 °C, and above this temperature the fcc-(Co,Pt) solution is expected.[26] Thus once again, the phase observed in the Co-Pt alloy clusters represents a state at a high temperature, even though the clusters were deposited at room temperature.

IV. DISCUSSION

A. General remarks

We have demonstrated that alloy clusters can be formed using the gas-aggregation technique, and that the use of two separate sputtering targets as sources of metal vapors helps control the composition of the produced clusters. The advantages of this method over a conventional evaporation technique include (i) ease of obtaining a wide range of materials: vapors of a substance with a high melting point, e.g., refractory metals, and even carbon vapors, can be generated, (ii) ease of controlling composition: the amount of a vapor is basically proportional to the amount of power applied to the target, and (iii) reproducibility: unlike conventional evaporation techniques, where the amount of a metal vapor is a sensitive function of the crucible temperature and the amount of materials inside the crucible, source materials are practically unlimited with sputter-based gas-aggregation techniques, and operational simplicity ensures reproducibility.

On the other hand, this technique does not change the basic processes of cluster formation in the gas phase. It is an irreversible reaction, and the resultant clusters are often in a metastable state. In our experiment, B2-typye Co-Al alloy clusters were observed in a composition range wider than that predicted by the phase diagram; the Co-Pt alloy possessed the fcc structure. These findings may be compared, for example, to the well-known occurrence of the A15 structure in Cr clusters produced by conventional gas-aggregation techniques.[35] In addition to the non-equilibrium aspect of the cluster-forming process, size is also a factor pertinent to clusters. Their small size, and consequently large surface-to-volume ratio, may explain their different structure from their bulk counterparts. At present, we cannot clearly show to
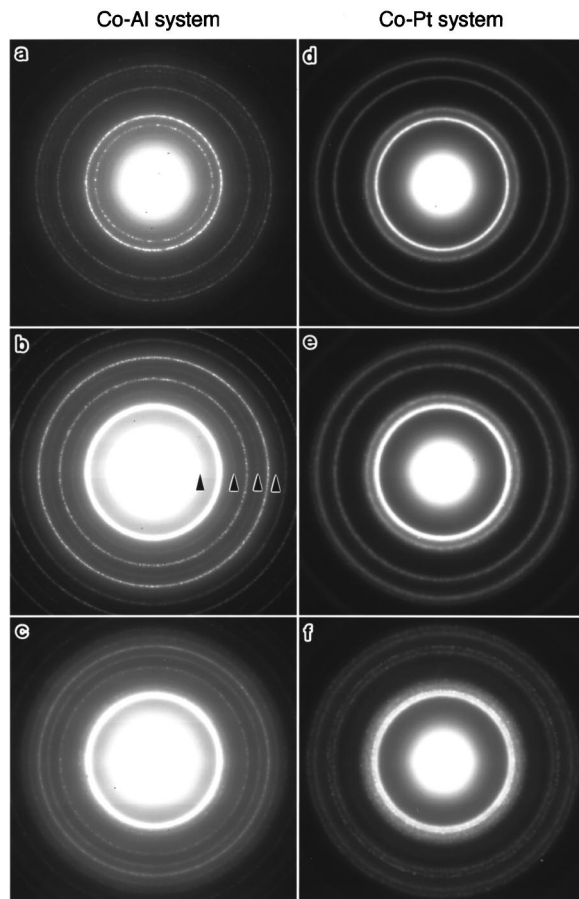
what degree the structure of the clusters were affected by the rapid quenching and by the smallness of their size. Below, we will briefly discuss the mechanism of alloy cluster formation based on a semiquantitative description of gas dynamics, and show the main cause of the observed differences between CoAl and CoPt clusters. For the sake of simplicity, we will focus on a cluster with a composition ratio of approximately Co:M=1:1.

We have seen that the size of the CoM (M=Al or Pt) alloy clusters at Co:M=1:1 composition is about 12 and 7 nm in diameter for Co-Al and Co-Pt systems, respectively. Knowing that they are made up with B2 ($a=2.86$ Å)[27] and Al (i.e., fcc; $a=3.54$ Å) phases,[28] respectively, we can estimate the number of atoms in these clusters. There are about 4×10^4 Co and Al atoms in the former, and 8×10^3 Co and Pt atoms in the latter. Thus, Co and M (Al or Pt) atoms were ejected from the targets, reacted in the gas phase, out of which the aforementioned numbers of atoms formed an alloy cluster resulting in a monodispersive size distribution.

B. Departure of cluster size distribution from LND

We first note that the size of alloy clusters does not follow LND, $f_{LN}(x)$, which is commonly known to occur for a number of small particle systems[15,36]

$$f_{LN}(x) = \frac{1}{\sqrt{2\pi} \ln \sigma} \exp\left\{ -\frac{1}{2}\left(\frac{\ln x - \ln \bar{x}}{\ln \sigma}\right)^2 \right\} \quad (2)$$

but obey the normal Gaussian distribution, $f_G(x)$:

$$f_G(x) = \frac{1}{\sqrt{2\pi} \sigma} \exp\left\{ -\frac{1}{2}\left(\frac{x - \bar{x}}{\sigma}\right)^2 \right\}, \quad (3)$$

where $\bar{x}$ and σ are the mean value and standard deviation, respectively. Some of the differences and similarities in the appearance of the two distribution functions is briefly discussed in the Appendix.

In the statistical theory of coalescence, LND arises when particles or clusters are formed by a certain number of random collisions and coalescences, in which the increase in volume is randomly distributed. This assumption of the random fractional increase in volume after collision, when the central limit theorem is applied, leads to LND.[16,36] Thus, the observed departure from LND as observed in Figs. 3(c)–3(j) strongly suggests that coalescence is not a dominant mechanism for cluster growth. In fact, Hihara and Sumiyama, in a study of Ni cluster formation, pointed out that collision coalescence does not explain a highly monodispersed cluster size distribution, and suggested monomer absorption should be the dominant mechanism.[37] They also suggested that clusters should be extracted from the growth chamber before they collide with each other.

Within the framework of monomer absorption, LND can take place if we assume that the growth rate is proportional to the volume of a cluster, ν. Namely,

$$d\nu/dt = K\nu, \quad (4)$$

where K is a kinetic constant. This leads to

$$t = 1/K \ln \nu + \text{const.} \quad (5)$$

If we now assume that the number of particles nucleated at a particular time t obeys Gaussian distribution, we will obtain LND.[38] This assumption is applicable when particles are formed in a stationary environment, such as colloid formation in a liquid phase or formation of small particles in a stagnant gas phase. In our case, clusters are formed in a flowing gas in a discrete time period, and thus, the assumption of Gaussian distribution for each cluster's history is not fulfilled. On the other hand, the size distribution of clusters rich in Al [Figs. 3(a) and 3(b)] do follow LND, as characterized by the long tail beyond the average value. This is partly due to heterogeneous structures of Al-rich clusters brought about by an excessive Al gas, which disturbed the condition of the discrete lifetime of clusters, and was discussed separately.[33]

In short, LND arises either when clusters are formed by a discrete number of collisions with a random selection of the fractional volume increase in each coalescence event or when clusters are formed by monomer absorption with a randomly distributed time period from the incipiency of each cluster. The fact that the observed cluster size distribution in the present article does not follow LND strongly suggests that these two mechanisms are not operational in the present method, but that the alloy clusters were formed by a substantially different mechanism. In view of these considerations, we will restrict the following qualitative discussion of alloy cluster formation to the framework of a monomer absorption mechanism with a discrete (not a Gaussian) distribution of time for growth.

C. Estimation of the number of collisions of metal atoms

First, the basic parameters that characterize a vapor phase must be identified. These include number density of Ar n_{Ar}; collision frequency of atoms f; residence time τ, and rough estimate of throughput of Ar gas Q_{Ar}, and metal vapor Q_M. Since the sputtering was carried out in an Ar atmosphere of approximately 130 Pa at room temperature, we have

$$n_{Ar} \approx 3.5 \times 10^{16} \ (\text{cm}^{-3}). \quad (6)$$

The average velocity c and mean-free-path λ are 3.9×10^2 m/s and 80 μm, respectively.[32] Thus, the collision frequency is given by

$$f = c/\lambda = 5 \times 10^6 \ (\text{s}^{-1}). \quad (7)$$

The residence time of an atom inside the chamber before it is escaped out of the growth region is given by

$$\tau = pV/(Q_{Ar} + Q_M) \approx pV/Q_{Ar}, \quad (8)$$

where p is the pressure inside the chamber, V the volume of the chamber, Q_{Ar} the throughput (flow rate) of the gas (which is much larger than Q_M). With $p=130$ Pa, $V=9 \times 10^3$ cm³, $Q=300$ sccm we have

$$\tau \approx 2.4 \ \text{s.} \quad (9)$$

We then need to estimate the relative amount of metal vapors inside the chamber. This can be done once we determine the sputtering yield of the metals. The values for 500 eV Ar ions are given in Table II. In our experiment, the applied voltage was about 300 V, and thus, the energy of Ar^+ was approximately 300 eV. Since this is larger than the threshold energy and given that the sputtering yield tends to increase with incident energy in this energy range,[39] we may determine that the sputtering yield is in the order of 0.3 atoms/ion. As a typical value for the applied current, I, we may set $I \approx 0.5$ A. Neglecting the effect of secondary electron production on the target, we may use this number as total Ar^+ flux on the 7-cm-diam target to make a rough estimation. Then, the number of metal atoms "injected" inside the chamber is approximately

$$Q_M \approx 5 \times 10^7 \; s^{-1}. \tag{10}$$

This is the "throughput" of the metal vapor.

Comparing Q_M with Q_{Ar}, we now know that the ratio of metal atoms to Ar atoms θ is approximately

$$\theta \approx Q_M / Q_{Ar} \approx 5 \times 10^{-3}. \tag{11}$$

That is, approximately one out of hundreds of atoms in the gas is either Co or M (Al or Pt) atoms. θ can also be regarded as the average probability of any atom meeting a metallic atom inside the chamber. It should be emphasized, however, that this value will be larger near the targets, and will decrease rapidly as the clusters grow.

These considerations suggest that each metal atom collides with hundreds of Ar atoms before it meets the same or other kinds of metal atoms. Even though the cooling efficiency of Al and Pt is different by a factor of two (Table II), it is reasonable to assume that these metals are thermalized quickly by the collisions with Ar atoms before they meet with another metal. In other words, we may, for the purpose of the present estimation, presume that the Ar atmosphere acts as a heat reservoir.

Next, we need to estimate the total number of collisions N_C between the metals before they are ejected from the growth region. This is in principle the product of the residence time and collision frequency with a metal (the latter is given by $\theta \times f$):

$$N_C \approx \tau \times \theta \times f \approx 6 \times 10^4. \tag{12}$$

We therefore see that N_C is in the same order as the number of atoms in CoAl. Needless to say, this is a very rough estimate since the density of metal vapors decreases rapidly as the cluster grows inside the vapor phase. But this is partially compensated by the increase of cross section σ for each collision since σ varies as

$$\sigma \approx r^2 \approx N^{2/3}, \tag{13}$$

where r is the radius and N is the total number of atoms of the cluster.[32]

D. Estimation of the sticking probability in Co-Al and Co-Pt systems

The above simple observation suggests that the number of collisions of metals in Co-Al and Co-Pt systems does not differ appreciably. This leads us to conclude that the observed size difference arises because the probability of the metal atoms arriving on a growing cluster staying there, i.e., sticking probability, differs appreciably between the two systems. In other words, CoPt is smaller than CoAl since the metal atom detaches from the cluster due to its low driving force for compound formation.

Provided that there is a sufficient number of collisions with Ar atoms, as discussed previously, we may assume that the atoms and growing clusters are in equilibrium with the heat reservoir. Thus, we may write

$$Co + M = CoM, \quad \Delta G^0_{CoM}, \tag{14}$$
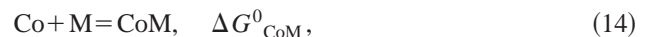
where ΔG^0_{CoM} is the standard free-energy change upon the formation of the compound phase, CoM. The equilibrium constant k_{CoM} is given by

$$k_{CoM} = p_{CoM}/(p_{Co}p_M) = \exp(-\Delta G^0_{CoM}/RT), \tag{15}$$

where p denotes the partial pressure. In the present article, we are interested in the ratio of the equilibrium constant in the Co-Al and Co-Pt systems.

For that purpose, we can neglect the effect of the entropy change ΔS, because it comprises mostly the change from gaseous to solid state, which is in the same order for both Co-Al and Co-Pt systems. With the enthalpy change tabulated in Table I, we obtain, at $T = 20\,°C$:

$$k_{CoAl} \approx \exp(-\Delta H_{CoAl}/RT) \approx 3 \times 10^{10}, \tag{16a}$$

$$k_{CoPt} \approx \exp(-\Delta H_{CoPt}/RT) \approx 1 \times 10^1. \tag{16b}$$

These are thermodynamical numbers that have significance only when a dynamical equilibrium between the left- and right-hand sides of the reaction equation exists. However, we may use the ratio of these values as a relative probability of the reaction to proceed towards the right-hand side of the equation. We see that Co and Al have a much larger probability of forming CoAl than Co and Pt do once they meet. In other words, Co and Pt may detach or reevaporate from Co-Pt alloy clusters, giving rise to a slow growth rate.

It should be emphasized here that the aforementioned rudimentary thermodynamical arguments only compare the relative stability of CoAl with that of CoPt. In this naive treatment, it is doubtful that the dynamical equilibria between the elemental metallic gas and clusters, as expressed by Eqs. (16a) and (16b), exist at room temperature. We may suggest however that, in the pioneering work by Riley[9] and Parks et al.,[40] it was demonstrated that phase equilibria do exist in the adsorption reactions between Ni and N_2 molecules in the temperature range of -122 to $50\,°C$, as appeared as a plateau in the composition-pressure curve for N_2 uptake by Ni clusters.[41] The systems investigated here were metallic, and thus may not be compared directly with the results obtained for the adsorption reaction. Yet the observed significant difference in the average size of the CoAl and

CoPt particles do suggest that the probability of a reaction going toward the right-hand side of Eq. (14) in the gas phase is strongly influenced by the thermodynamical character of the system.

Overall, our results indicate that it is possible to obtain monodispersive alloy clusters (as opposed to LND) from two separate elemental sputtering sources, provided that these metallic vapors can meet and be cooled effectively in a gaseous phase, and have a discrete residence time inside the chamber. The resultant clusters, however, are not in a state of free-energy minimum. Yet it was shown that the thermodynamical property of the alloy system influences the growth rate, and thereby, the average size of the produced alloy clusters.

V. CONCLUSIONS

We employed a plasma-gas-aggregation technique to synthesize Co-Al and Co-Pt alloy clusters. Our apparatus was characterized by two separate elemental sputtering sources, high-Ar pressure ($\approx$130 Pa), and a growth region. The composition of the alloy clusters could easily be controlled, and their size distribution was found to be monodispersive. However, the composition and size of the clusters are not uniquely functions of the power supplied to the two targets, but they also depend critically on the thermodynamics of the system, as well as on kinetic factors such as the flow rate of the carrier gas. Thus, in the Co-Al system, monodispersed intermetallic alloy clusters of CoAl with B2 structure were formed for a composition range wider than that predicted by the equilibrium phase diagram; whereas in the Co-Pt system, CoPt alloy clusters formed the fcc phase, which is a metastable phase at room temperature. The average size of CoAl was about 12 nm, while that of CoPt was about 7 nm in diameter under identical conditions. Therefore, even though the alloys formed in the gaseous phase are in a metastable state, the thermodynamical properties of the system are still a dominant factor governing their growth rate, and thus their size.

ACKNOWLEDGMENT

APPENDIX

The log-normal distribution function (LND), $f_{LN}(x)$, can be distinguished from the normal Gaussian function, $f_G(x)$, by its asymmetric shape, i.e., by a long tail in the large x region. From a viewpoint of cluster growth, this is a consequence of either (i) statistical theory of coalescence, or (ii) volume-dependent growth rate, as discussed in the text. In Fig. 7, we can compare these two functions for several different standard deviation σ values. Besides the asymmetry in LND when σ is large, it can be noticed that these two functions are practically indistinguishable when σ approaches to a small value, as can be seen from $f_{LN}(x)$ with $\sigma=1.08$. If
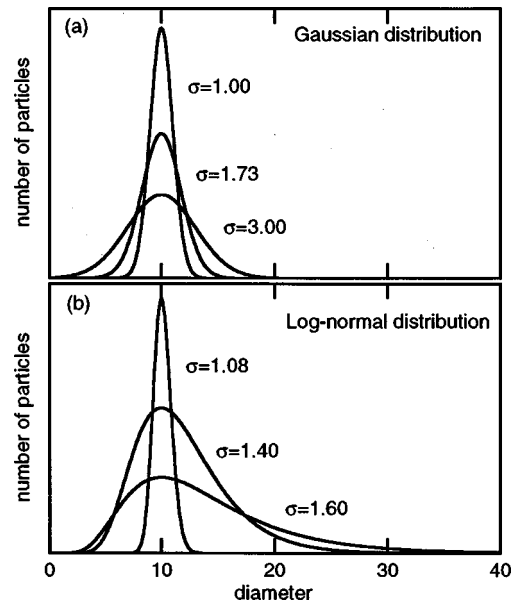

FIG. 7. Comparison of the appearance of (a) Gaussian distribution and (b) LND for the average value of $\bar{x}=10$ and several values of standard deviation σ. The LND is characterized by its long tail. Note that, when s is small, the two distributions are indistinguishable.

this happens, it is no longer physically desirable to call such a distribution LND, and we lose physical footings for the aforementioned models for LND, even though it may still mathematically be LND.

The corollary of this argument is that one should not invoke LND when a size distribution in question does not demonstrate asymmetry, as characterized by a long tail beyond the average value within a given experimental precision. This was seen in the distributions in Figs. 3(c)–3(j), and they should be fitted by the normal Gaussian function, not by LND.

[1]A. H. Pfund, Phys. Rev. **35**, 1434 (1930).
[2]L. Harris, D. Jeffries, and B. M. Siegel, J. Appl. Phys. **19**, 791 (1948).
[3]K. Kimoto, Y. Kamiya, M. Nonoyama, and R. Uyeda, Jpn. J. Appl. Phys. **2**, 702 (1963).
[4]J. D. Eversole and H. P. Broida, J. Appl. Phys. **45**, 596 (1974).
[5]C. Hayashi, J. Vac. Sci. Technol. A **5**, 1375 (1987).
[6]C. Bréchignac, P. Cahuzac, F. Carlier, M. de Frutos, A. Masson, and J. P. Roux, Z. Phys. D: At., Mol. Clusters **19**, 195 (1991).
[7]P. Milani and W. A. deHeer, Rev. Sci. Instrum. **61**, 1835 (1990).
[8]H. Haberland, M. Karrais, M. Mall, and Y. Thurner, J. Vac. Sci. Technol. A **10**, 3266 (1992).
[9]S. J. Riley, J. Non-Cryst. Solids **205−207**, 781 (1996).
[10]S. Yamamuro, K. Sumiyama, and K. Suzuki, J. Appl. Phys. **85**, 483 (1999).
[11]C. Kaito, Jpn. J. Appl. Phys. **17**, 601 (1978).
[12]J. M. Soler, N. García, O. Echt, K. Sattler, and E. Recknagel, Phys. Rev. Lett. **49**, 1857 (1982).
[13]F. Frank, W. Schulze, B. Tesche, J. Urban, and B. Winter, Surf. Sci. **156**, 90 (1985).
[14]W. Knauer, J. Appl. Phys. **62**, 841 (1987).
[15]J. L. Katz, J. Chem. Phys. **52**, 4733 (1970).
[16]C. G. Granqvist and R. A. Buhrman, J. Appl. Phys. **47**, 2200 (1976).
[17]Y. Saito, K. Mihama, and R. Uyeda, Jpn. J. Appl. Phys. **19**, 1603 (1980).
[18]K. Sattler, J. Mühbach, and E. Recknagel, Phys. Rev. Lett. **45**, 821 (1980).
[19]C. Kaito, K. Fujita, H. Shibahara, and M. Shiojiri, Jpn. J. Appl. Phys. **16**, 697 (1977).
[20]R. W. Siegel, S. Ramasamy, H. Hahn, L. Zongquan, L. Ting, and R. Gronsky, J. Mater. Res. **3**, 1367 (1988).

[21] N. Yukawa, M. Hida, T. Imura, M. Kawamura, and Y. Mizuno, Metall. Trans. **3**, 887 (1972).

[22] T. Yogi and T. A. Nguyen, IEEE Trans. Magn. **29**, 307 (1993).

[23] S. Gangopadhyay, G. C. Hadjipanayis, C. M. Sorensen, and K. J. Klabunde, IEEE Trans. Magn. **29**, 2602 (1993).

[24] Y. Wang, Y. X. Li, and K. J. Klabunde, *ACS Sym. Series.*, Vol. 517, edited by M. E. Davis and S. L. Suib (American Chemical Society, Washington, DC, 1993), pp. 136–155.

[25] A. J. McAlister, in *Binary Alloy Phase Diagrams*, 2nd ed., edited by T. B. Massalski (ASM International, Materials Park, 1990), pp. 136–138.

[26] T. B. Massalski, in *Binary Alloy Phase Diagrams*, 2nd ed., edited by T. B. Massalski (ASM International, Materials Park, 1990), pp. 1225–1226.

[27] *Pearson's Handbook of Crystallographic Data*, 2nd ed. (ASM International, Materials Park, 1991), pp. 716–717.

[28] *Pearson's Handbook of Crystallographic Data*, 2nd ed. (ASM International, Materials Park, 1991), pp. 2551–2552.

[29] F. R. de Boer, R. Boom, W. C. M. Mattens, A. R. Miedema, and A. K. Niessen, in *Cohesion in Metals Transition Metal Alloys* (North-Holland Amsterdam, 1988).

[30] S. Yamamuro, M. Sakurai, K. Sumiyama, and K. Suzuki, in *Similarities and Differences Between Atomic Nuclei and Clusters*, edited by Y. Abe, I. Arai, S. M. Lee, and K. Yabana, AIP Conf. Proc. No. 416 (AIP, New York, 1998), p. 491.

[31] J. L. Vossen and W. Kern, in *Thin Film Processes* (Academic, New York, 1978), p. 15.

[32] B. Chapman, in *Glow Discharge Processes* (Wiley, New York, 1980).

[33] T. J. Konno, Y. Yamamuro, and K. Sumiyama, J. Appl. Phys. **90**, 3079 (2001).

[34] J.-J. Delaunay, T. Hayashi, M. Tomita, S. Hirono, and S. Umemura, Appl. Phys. Lett. **71**, 3427 (1997).

[35] K. Kimoto and I. Nishida, J. Phys. Soc. Jpn. **22**, 744 (1967).

[36] C. G. Granqvist, J. Phys. Colloq. **7**, C2-147 (1977).

[37] T. Hihara and K. Sumiyama, J. Appl. Phys. **84**, 5270 (1998).

[38] R. R. Irani, J. Phys. Chem. **63**, 1603 (1959).

[39] P. Sigmund, Phys. Rev. **184**, 383 (1969).

[40] E. K. Parks, G. C. Nieman, and S. J. Riley, J. Chem. Phys. **115**, 4125 (2001).

[41] I. K. Parks, L. Zhu, and S. J. Riley, J. Chem. Phys. **102**, 7377 (1995).